NiTi Belleville washers: Design, manufacturing and testing

3 authors:

Carmine Maletta
Università della Calabria
130 PUBLICATIONS **2,240** CITATIONS

SEE PROFILE

Franco Furgiuele
Università della Calabria
68 PUBLICATIONS **989** CITATIONS

SEE PROFILE

Letícia de Souza Castro Filice
159 PUBLICATIONS **4,537** CITATIONS

SEE PROFILE

NiTi Belleville washers: Design, manufacturing and testing

Carmine Maletta, Luigino Filice and Franco Furgiuele

Abstract

The thermomechanical properties of nickel–titanium-based Belleville washers have been analyzed in this investigation, together with their unusual mechanical and functional features, which can be attributed to the reversible phase transformation mechanisms of nickel–titanium alloys. In particular, numerical simulations have been carried out for a preliminary design of the Belleville washer, using a commercial finite element software and a special constitutive model for shape memory alloys. Subsequently, Belleville washers have been manufactured from a commercial pseudoelastic nickel–titanium alloy, by disk cutting and a successive shape setting by a thermomechanical treatment. Finally, the thermomechanical response of the washers, in terms of isothermal force–deflection curve and thermal cycles between phase transition temperatures, has been experimentally analyzed. The results highlighted a marked effect of the temperature on the characteristic curve, as well as good recovery capabilities under both mechanical and thermal cycles. In addition, nickel–titanium Belleville washers exhibit a marked hysteretic behavior, as a consequence of the hysteresis in the stress–strain response of the alloy. Thanks to these features, nickel–titanium Belleville washers can be used as smart elastic elements, that is, with tunable stiffness and damping properties, as well as solid-state actuators, due to their recovery capabilities.

Introduction

Nickel–titanium (NiTi)-based shape memory alloys (SMAs) are currently used for the realization of smart and/or active components in many fields of engineering and medicine (Otsuka and Wayman, 1998), thanks to their unique functional properties, namely, shape memory effect (SME) and pseudoelastic effect (PE), as well as to their good mechanical performances and biocompatibility (Otsuka and Ren, 2005). Nevertheless, despite this technological interest, the use of NiTi alloys is currently limited to high-value applications due to the complex material processing and manufacturing, as the functional and mechanical behaviors are strongly affected by the thermomechanical loading history, experienced during manufacturing and even during service. However, the demand for these alloys is constantly increasing, and consequently, a continuous improvement in product quality and a reduction in manufacturing costs are expected in the near future. As a direct consequence of this trend, the use of NiTi alloys is expected to move from niche engineering and biomedical markets to mainstream engineering applications. In this framework, several scientific and technological research activities have been carried out in the last few years with the aim of exploiting new NiTi-based devices and components to be used in common engineering applications. In particular, the use of NiTi alloys for the realization of smart springs offers very interesting features, such as high recovery capabilities, temperature-dependent properties, active and/or tunable response, and high damping properties, thanks to the reversible stress-induced martensite (SIM) and/or thermally induced martensite (TIM) phase transformation. The properties of such springs have been exploited for the realization of actuators (Reynaerts and Van Brussel, 1998), vibration and seismic absorbers (Saadat et al., 2002), orthodontic springs (Wichelhaus et al., 2010), etc. In particular, NiTi-based helical springs have been deeply investigated, and advanced spring designs with hollow cross section have been also proposed (Spinella and Dragoni, 2010; Spinella et al., 2010), with the aim to reduce the heating and cooling time with respect to the solid section; in fact, this feature is of major concern

Department of Mechanical Engineering, University of Calabria, Arcavacata di Rende, Italy

Corresponding author:
Carmine Maletta, Department of Mechanical Engineering, University of Calabria, Ponte P. Bucci 44C, 87036 Arcavacata di Rende, Italy.
Email: carmine.maletta@unical.it

if dealing with active elements to be used in actuation systems. Furthermore, some research activities have been also devoted to the study of mechanical and functional properties of SMA-based Belleville springs (Labrecque et al., 1996; Speicher et al., 2009; Trochu and Terriault, 1998). In particular, the load–deflection curve of a SMA Belleville washer for electrical applications has been numerically analyzed in Trochu and Terriault (1998), and the temperature-dependent response of a CuAlNiMnTi-based washer has been analyzed in Labrecque et al. (1996). More recently, Belleville washers have been used to develop a device for seismic retrofit of buildings (Speicher et al., 2009), which demonstrated interesting and exploitable damping properties. However, much research should be carried for a better understanding of the complex thermomechanical response of SMA-based Belleville washers, as well as for their manufacturing processes starting from commercially available raw materials. To this aim, numerical simulations have been carried out, using a commercial finite element (FE) software and a special constitutive model for SMAs (Auricchio, 2001; Auricchio and Taylor, 1997), for a preliminary design of the Belleville washer, as well as to analyze their thermomechanical response. Subsequently, Belleville washers have been manufactured from a commercial pseudoelastic Ni-rich NiTi sheet, by mechanical shearing and successive high temperature forming (823 K for 30 min) using a properly designed stainless steel die. Moreover, the thermomechanical response of the washers, in terms of force–deflection curve and thermal cycles between phase transition temperatures, has been experimentally analyzed. In particular, the isothermal mechanical response of the spring, that is, the force versus deflection curve, has been analyzed under different values of the temperature, and the deflection recovery capabilities under thermal cycles, between the phase transition temperatures, have been investigated. These investigations revealed a marked effect of the temperature on the thermomechanical response of the washer, that is, they highlighted variable properties in terms of both stiffness and shape recovery, when varying the temperature in the range between 298 and 403 K. Finally, as expected, differential scanning calorimetry (DSC) investigations of the as-received material and the thermally treated one revealed a marked modification of the thermomechanical properties, in terms of phase transition temperatures as a consequence of the thermomechanical forming process.

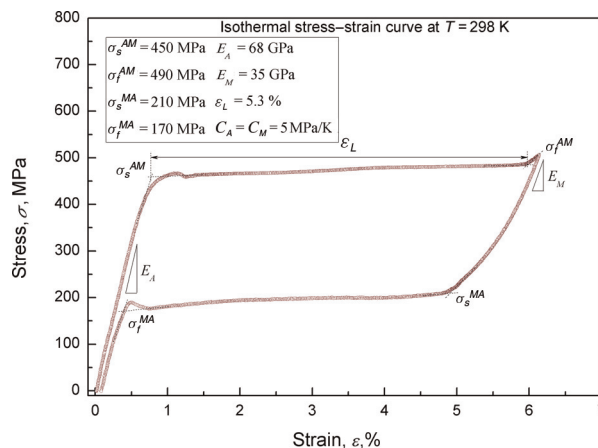## Material properties and preliminary design of the washer

In the following subsections, the thermomechanical properties of the investigated commercial pseudoelastic alloy are first reported, and subsequently, a preliminary design of the Belleville washer is illustrated, which was carried out using a commercial FE software and a special constitutive model for SMAs. In addition, the role of phase transition mechanism on the characteristic load–deflection curve of the washer has been analyzed.
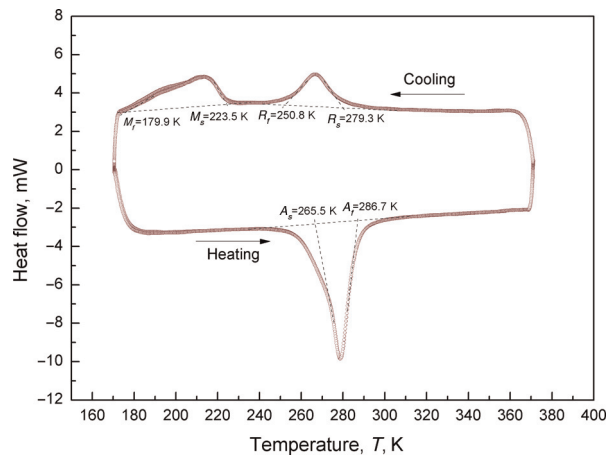
Material properties

A commercial pseudoelastic NiTi sheet (Type S, Memory-Metalle, Germany), with nominal chemical composition of $50.8\,at.\%\,Ni - 49.2\,at.\%\,Ti$ and with thickness of $t = 1.5\,mm$, has been used in this investigation. The raw material has been analyzed by thermomechanical tests and DSC investigations. In particular, dog bone–shaped specimens were made by electro discharge machining, and the thermomechanical tests were carried out using a universal testing machine (Instron, Model 8500) equipped with an environmental chamber (MTS, Model 651) and a resistance extensometer to measure the local deformations of the specimens. Furthermore, a MTS TestStar II controller was used for simultaneous acquisition and/or control of load, deformation, and temperature. Figure 1 illustrates a stress–strain curve of the material, obtained from an isothermal ($T = 298\,K$) displacement-controlled loading–unloading cycle up to a maximum deformation of $\varepsilon = 6.2\%$, corresponding to the maximum deformation of the stress–strain transformation plateau. Furthermore, Figure 1 shows the values of the main mechanical parameters of the alloy, in terms of Young's moduli (E_A and E_M), transformation stresses (σ_s^{AM}, σ_f^{AM}, σ_s^{MA}, and σ_f^{MA}), and transformation strain (ε_L), together with the Clausius–Clapeyron constant ($C_A = d\sigma^{MA}/dT$ and $C_M = d\sigma^{AM}/dT$), which were obtained from isothermal tests carried out at different values of the temperature.

Figure 2 illustrates the DSC thermogram of the raw material, which was obtained at a heating/cooling rate

Figure 1. Measured isothermal stress–strain curve and thermomechanical parameters of the investigated NiTi alloy.
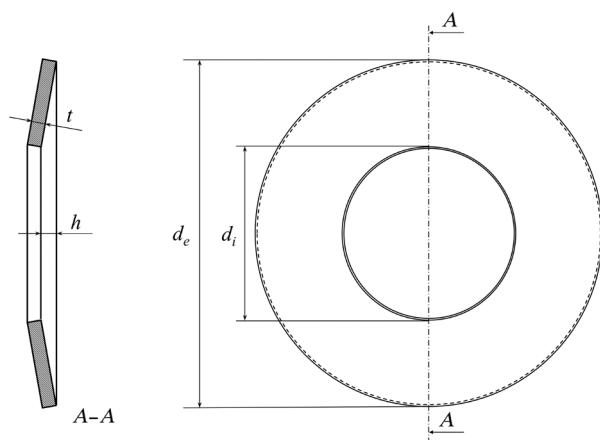NiTi: nickel–titanium.

Figure 2. DSC thermogram of the investigated NiTi alloy.
DSC: differential scanning calorimetry; NiTi: nickel–titanium.

of $1.6\,\mathrm{K\,s^{-1}}$. The DSC curve shows that the material exhibits a rhombohedral (R)-phase transformation during cooling prior to the martensitic transformation. Furthermore, Figure 2 shows the values of all transformation temperatures (M_s, M_f, A_s, A_f, R_s, and R_f). However, the A–R transformation is not noticeable in the stress–strain curve of Figure 1, maybe because it occurs just below the martensitic transformation stress, and it can be attributed to a slight change of the slope of the stress–strain curve.

Preliminary design of the NiTi-based Belleville washer

Belleville washers are characterized by a conical shape that provides a unique mechanical response if compared with more traditional helical springs, that is, they exhibit a nonlinear and/or nonmonotonic load–deflection response. Figure 3 illustrates a schematic depiction of a Belleville washer together with the main geometrical parameters, that is, the outer and inner
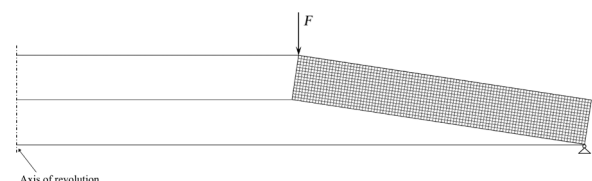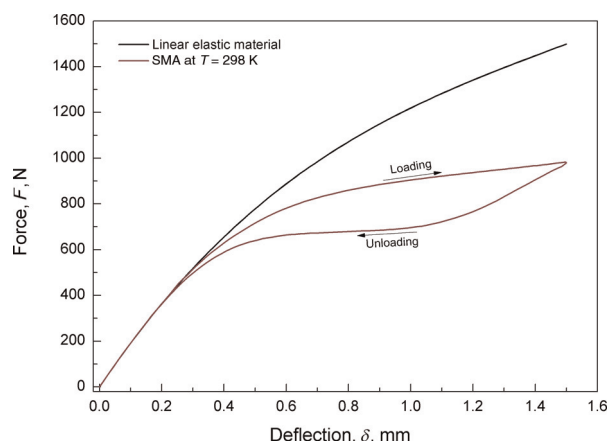
diameters, d_e and d_i, respectively, the cone height h, and the thickness t. Normally, the load versus deflection curves of such springs are given as a function of two non-dimensional geometrical parameters: the ratios h/t and d_e/d_i; the variation of these parameters produces a wide variety of nonlinear load–deflection curves and, in particular, when increasing the ratio h/t, a nonmonotonic response could be obtained involving a snap-action mechanism. In addition, the use of NiTi-based SMAs for the realization of Belleville springs is expected to produce more complex load–deflection curves with respect to common metals, as a direct consequence of the unique constitutive behavior of such alloys, that is, of the stress-induced phase transformation mechanisms. For a better understanding of the thermomechanical behavior of NiTi-based Belleville washers, preliminary numerical studies have been carried out using a commercial FE software (MSC Software, Marc) and a special constitutive mechanical model for SMAs (Auricchio, 2001; Auricchio and Taylor, 1997). These studies allowed to obtain a preliminary design of the spring, that is, several simulations have been carried out to define the geometry of the washer, in terms of h/t and d_e/d_i ratios. In particular, these latter were chosen to avoid a nonmonotonic characteristic curve at room temperature, and the following values have been selected: $d_e/d_i = 2$ and $h/t = 1$, with $d_i = 20\,\mathrm{mm}$ and $t = 1.5\,\mathrm{mm}$.

Numerical simulations were carried out using 2D axisymmetric FE models, as illustrated in Figure 4. In particular, the model represents a cross section of the washer and consists of 1500 2D four-noded quadrilateral elements, subjected to axisymmetric loads and boundary conditions. A nonlinear analysis was carried out, and the deflection was simulated by two rigid compression plates, corresponding to the testing conditions, under the assumption of frictionless contact between washer and plates. Furthermore, the material parameters reported in the previous section have been adopted in the numerical simulations.

Figure 5 illustrates a comparison between the characteristic curves of a SMA at room temperature (298 K) and an equivalent elastic material having the same Young's modulus of the austenitic structure of the SMA ($E = 68\,\mathrm{GPa}$). Figure 5 clearly illustrates a similar response of the two materials for low values of the applied load, that is, for $F < 500\,\mathrm{N}$, due to a complete

Figure 3. Schematic depiction of a Belleville spring with the main geometrical parameters.

Figure 4. FE model of a cross section of the Belleville spring.
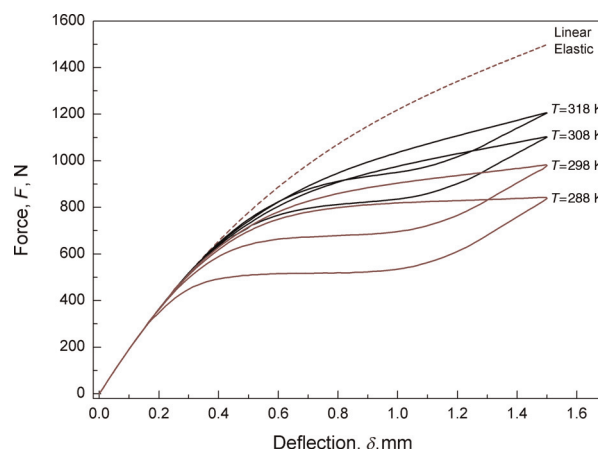FE: finite element.

Figure 5. Comparison of the characteristic curve for a SMA at room temperature (298 K) and an equivalent elastic material having the same Young's modulus of the austenitic structure of the SMA.
SMA: shape memory alloy.

Figure 6. Comparison of the characteristic curves for a SMA at different testing temperatures in the range of 288 − 318 K. SMA: shape memory alloy.

elastic response of the austenitic structure; if the load is further increased, the stress-induced martensitic transformation occurs and the SMA exhibits a smaller stiffness with respect to the elastic material, due to the stress–strain transformation plateau of the alloy. Furthermore, a great difference between the two materials arises when unloading, as the SMA shows a marked hysteretic behavior, that is, the unloading path is different from the loading one, as a direct consequence of the hysteresis associated with the reverse stress-induced martensitic transformation. This feature is particularly useful for the realization of vibration and/or seismic absorbers, as demonstrated in Speicher et al. (2009).

In addition, due to the temperature-dependent stress–strain response of NiTi alloys, by the Clausius–Clapeyron relation, this parameter is expected to play a significant role on the characteristic curve of NiTi-based Belleville springs. To this aim, several numerical simulations were carried out at different values of the temperature, and the force versus deflection curves have been analyzed, as illustrated in Figure 6, which reports a comparison between four isothermal loading–unloading curves in the temperature range of 288 − 318 K. Figure 6 clearly shows a similar response between the curves for low values of the applied force ($F < 300$ N), that is, where the SMA behaves like a linear elastic material, while a marked effect of the temperature is observed for higher values of the force in terms of both stiffness and hysteresis; in particular, when increasing the temperature, the force–deflection curve approaches that obtained from a linear elastic material, that is, the stiffness increases and the hysteretic behavior tends to vanish, as a direct consequence of the increase in the transformation stresses, according to the Clausius–Clapeyron relation, which in turn

causes an overall reduction of the stress-induced phase transformation mechanisms. On the contrary, marked hysteresis and flat force–deflection curves are obtained when decreasing the temperature, due to the formation of wide phase transformation regions. In any case, it is worth noting that the simulations were carried out by a simplified constitutive model for SMAs (Auricchio, 2001; Auricchio and Taylor, 1997), which does not take into account several microstructural mechanisms, such as martensite stabilization and yielding, and it is based on an initial fully austenitic structure, that is, it does not consider the presence of an initial martensite fraction. Furthermore, the same Young's modulus for the two phases of the material has been adopted ($E_A = E_M$), due to the constitutive model assumptions. However, the Young's modulus variation during stress-induced phase transformation, between E_A and E_M, is expected to play a significant role on the load/deflection curve of the spring. In addition, both martensite stabilization and initial volume fraction of martensite could be observed in the Belleville washer, especially when decreasing the testing temperature, resulting in residual displacements after unloading and, unfortunately, these mechanisms are not taken into account by the adopted numerical model. Due to these assumptions and limitations, as well as to the marked modification of the thermomechanical properties of the alloy after the thermomechanical forming process, a direct comparison between FE results and experimental measurements, reported in the following section, cannot be made. As a consequence, FE simulations can be just considered as preliminary studies that allow to define the overall geometric properties of the Belleville washers based on the design needs, but complete experimental tests should be carried out for an accurate knowledge of their thermomechanical response.

Spring manufacturing and experimental testing

In the following subsections, the manufacturing process to obtain NiTi-based Belleville washers from as-received NiTi sheets is first illustrated, and subsequently, the results obtained from the thermomechanical characterization of the spring are presented and discussed.
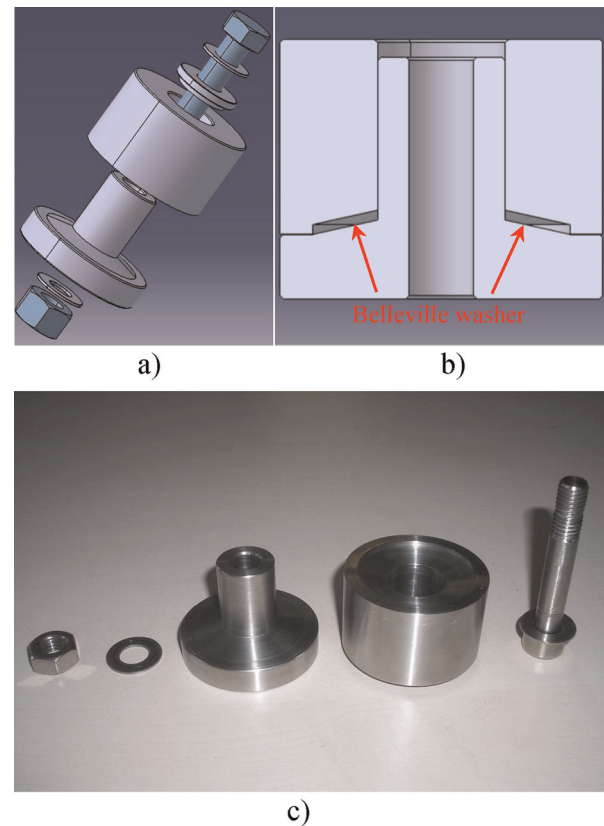
Spring manufacturing

NiTi-based Belleville washers have been manufactured, with geometrical parameters identified in the previous numerical studies ($d_e/d_i = 2$ and $h/t = 1$, with $d_i = 20$ mm and $t = 1.5$ mm), from as-received NiTi sheets with thickness of $t = 1.5$ mm, by the following two subsequent steps:

1. *Disk shearing*: Flat circular disks have been cut by wire electro discharge machining from the NiTi sheet;
2. *Shape setting*: A thermomechanical treatment was carried out for the shape setting of the spring, using a properly designed die.

In particular, a stainless steel die was made, as illustrated in Figure 7, which consists of two main parts assembled together by a bolt. In particular, Figure 7(a) illustrates a CAD assembly of the die, Figure 7(b) shows a diametral section, while the picture in Figure 7(c) illustrates all realized components of the die. As shown in Figure 7(b), the disk is positioned between the upper and lower parts of the die, and a load is applied, through the bolt, which deforms the disk in a conical shape, that is, to a shape closed to the target geometry of the spring. After that, a thermal treatment is carried out at an aging temperature of 823 K for 30 min and successive water quenching. In addition, preliminary experiments were carried out to choose the cone height of the die, equal to 2.25 mm, which allows to obtain a spring with the target cone height of $h = 1.5$ mm. In fact, complex springback mechanisms occur after thermomechanical treatments, due to both elastic response and phase transformation mechanisms.

Furthermore, Figure 7 illustrates that the die was designed to avoid a direct environmental exposure of the disk during thermal treatments, using a special joining design between the two parts. Figure 8 illustrates a picture of the flat disk after cutting (left) and of the Belleville spring after shape setting (right).

However, it is well known that functional properties of NiTi alloys are significantly affected by the thermomechanical loading history experienced during material processing and/or component manufacturing; therefore, a DSC test of the thermally treated material has been carried out, using a specimen directly obtained

Figure 7. Special die for shape setting of the NiTi-based Belleville spring: (a) CAD assembly, (b) diametral section, and (c) picture of the realized parts of the die.
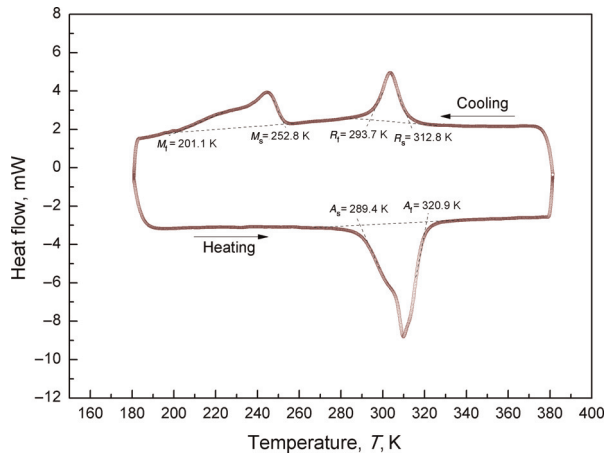NiTi: nickel–titanium.

Figure 8. Flat disk after sheet cutting (left) and Belleville spring after shape setting (right).

from a manufactured Belleville washer. Figure 9 illustrates the measured DSC thermogram of the thermally treated alloy, and a direct comparison with Figure 2 highlights a marked increase in the phase transition temperature with respect to the raw material. This is an expected result, which can be attributed to the formation of Ni-rich precipitates at high temperature (Otsuka and Ren, 2005) and, consequently, to the increase of Ti content in the alloy.

Thermomechanical characterization

The thermomechanical characterization of the manufactured washers was carried out using the same testing equipment described in section "Material properties." Furthermore, very low roughness and well-lubricated
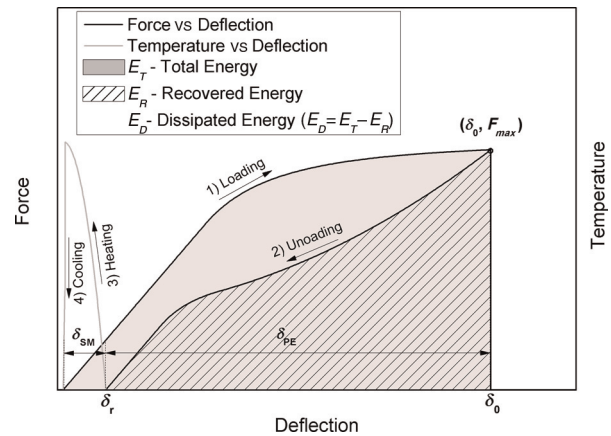
Figure 9. DSC thermogram of the thermally treated material.
DSC: differential scanning calorimetry.

Figure 10. Schematic depiction of the testing cycle carried out to study the thermomechanical response of the Belleville washers.

compression plates have been used to reduce friction during mechanical tests. The thermomechanical response of the manufactured NiTi-based Belleville springs has been measured by thermomechanical cycles composed of following four subsequent steps, as schematically depicted in Figure 10:

1. Isothermal displacement-controlled compression loading, at a testing temperature T_t and a displacement rate of 0.2 mm/min, up to a maximum deflection of $\delta_0 = 1.3$ mm, which is close to the maximum value of 1.5 mm (cone height of the washer), and recording the maximum force F_{max};
2. Isothermal displacement-controlled complete unloading at the same rate and temperature T_t, and measuring the mechanical recovery, which can be regarded as a pseudoelastic recovery δ_{PE}, and the residual deflection δ_r;
3. Heating up from the testing temperature T_t to the maximum temperature $T = 403$ K, at a heating rate of 2 K/min, to obtain a complete austenitic structure;
4. Cooling down to the testing temperature T_t at the same rate, to obtain the initial thermomechanical loading conditions of the spring and measuring the thermal recovery δ_{SM}, which can be attributed to the SME.

Note that in Figure 10, the residual deformations are assumed to be completely recovered after thermal cycle ($\delta_r = \delta_{SM}$); this behavior is normally observed when the material shows a stable functional response. To this aim, several transformation cycles have been applied to the manufactured washers in order to obtain a stable behavior, that is, with no irreversible effects after thermomechanical cycle; the results reported in the following have been obtained after complete
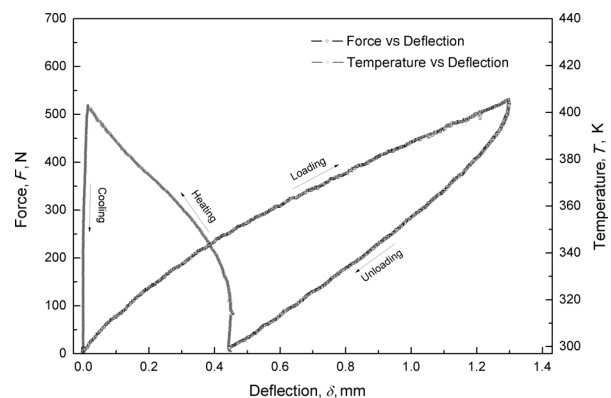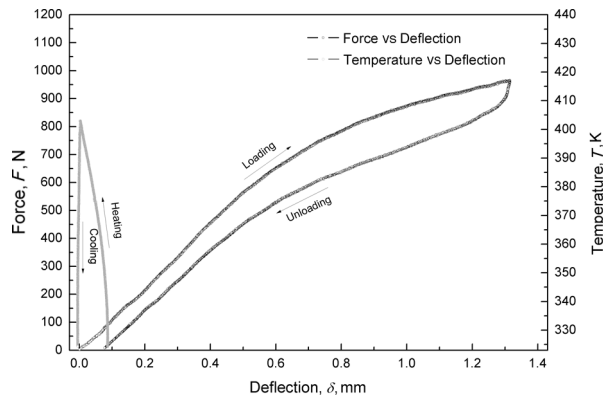
stabilization of the washer. Furthermore, some energetic parameters involved in the thermomechanical cycle have been computed, as illustrated in Figure 10: the total energy E_T, that is, the work associated with mechanical loading; the recovery energy E_R, that is, the energy recovered upon unloading due to the PE; and the dissipated energy E_D, which can be regarded as the energy of the load–deflection hysteresis loop, that is, the difference between total energy and recovered energy ($E_D = E_T - E_R$). Several tests have been carried out, as reported in section "Results and discussions," to study the thermomechanical response of the Belleville washer, by changing the value of the testing temperatures T_t in the range of $298 - 373$ K.

Results and discussions

Figure 11 illustrates the results obtained from the isothermal testing temperature $T_t = 298$ K and the subsequent thermal cycle. This figure also illustrates a marked loading–unloading hysteretic behavior with a significant
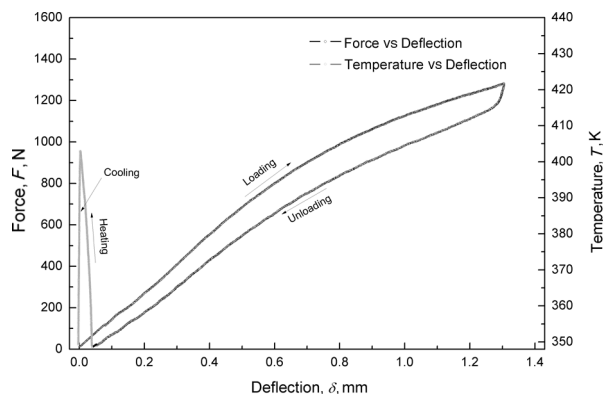

Figure 11. Isothermal load–deflection curve of the Belleville spring at $T_t = 298$ K and subsequent thermal cycle.
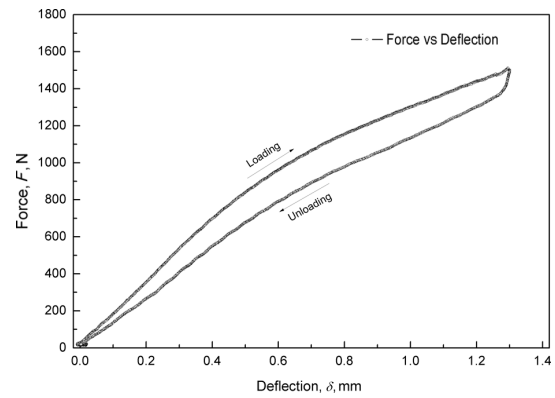
Figure 12. Isothermal load–deflection curve of the Belleville spring at $T_t = 323$ K and subsequent thermal cycle.

Figure 14. Isothermal load–deflection curve of the Belleville spring at $T_t = 373$ K.

residual deflection upon unloading, $\delta_r = 0.44$ mm, together with a low stiffness, with maximum force of about 530 N. Furthermore, the spring recovers its original shape after the thermal cycle between 298 and 403 K. In fact, the testing temperature $T_t = 298$ K is lower than the measured austenite finish temperature reported in Figure 9 ($A_f = 320.9$ K) and, consequently, a thermal cycle involving complete austenitic transformation must be carried to recovery the initial shape.

Figure 12 shows the characteristic curve of the spring at the test temperature $T_t = 323$ K; the comparison with Figure 11 shows a marked increase of the stiffness, with maximum force of about 960 N, and a much smaller hysteresis and residual deformation, with a deflection after unloading of about 0.08 mm. In particular, even if the testing temperature is slightly higher than the austenite finish temperature, a small residual deflection is observed, which can be attributed to a small amount of residual martensite variants that do not transform to parent phase after unloading, and a complete austenitic structure is observed only by an overheating far above A_f. In fact, the washer recovers its original shape when heating the spring up to 403 K. Similar considerations can be applied to Figure 13, which shows the results

relative to the testing temperature $T_t = 348$ K. In particular, in this case, a further increase of the stiffness is observed, with a maximum force of 1300 N and a residual deflection of 0.06 mm.

Finally, Figure 14 illustrates the mechanical tests carried out at $T_t = 373$ K, which shows a complete recovery of the spring upon unloading, and consequently, the thermal cycle is not carried out. In this case, a maximum force of about 1500 N is observed and the temperature is high enough for complete martensite to parent phase transformation after unloading, that is, a fully pseudoelastic response is observed.

For a better understanding of the evolution of both mechanical and functional properties of the Belleville washers, direct comparisons between the results obtained from the different thermomechanical tests have been carried out. In particular, in Figure 15, a comparison between the isothermal loading–unloading curves obtained at the investigated testing temperature is illustrated; this graph clearly shows the marked effect of the temperature on the characteristic curve of the

Figure 13. Isothermal load–deflection curve of the Belleville spring at $T_t = 348$ K and subsequent thermal cycle.

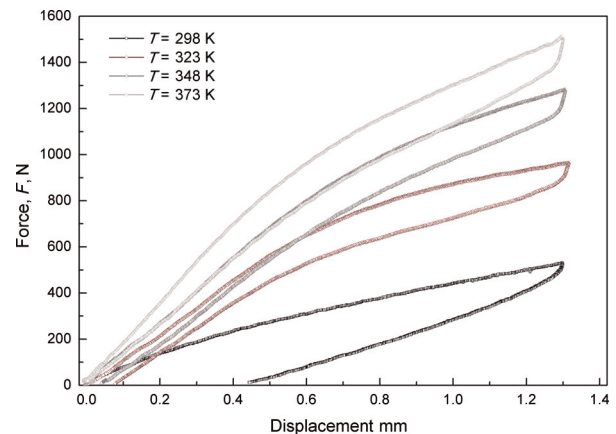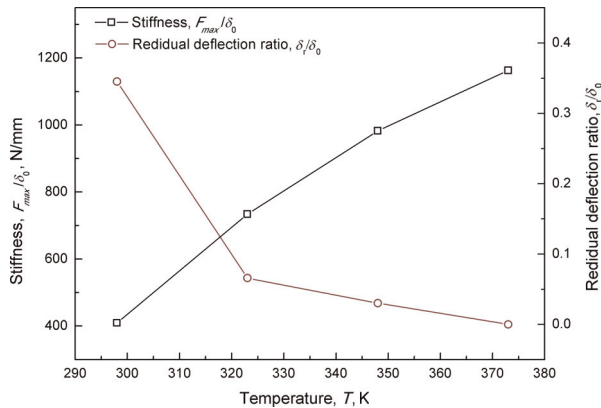**Figure 15.** Comparison of the isothermal load–deflection curve of the Belleville spring at different testing temperatures.

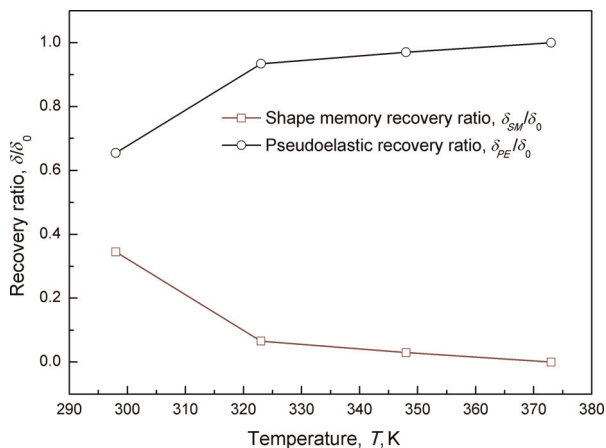**Figure 16.** Stiffness and residual deflection of the washer as a function of the testing temperature.

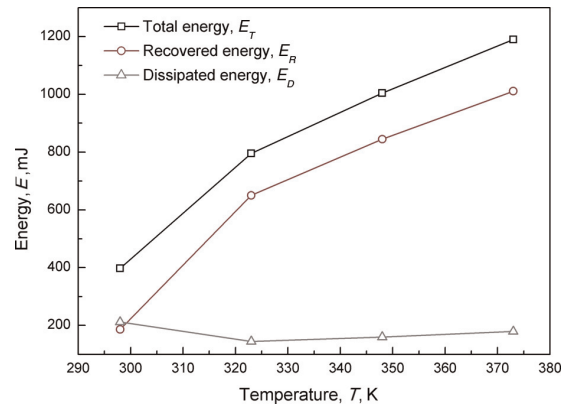**Figure 18.** Energetic parameters as a function of the testing temperature, T_t.

Belleville spring, in terms of stiffness, hysteretic behavior, and recovery capabilities.

Figure 16 illustrates the values of the stiffness at the maximum deflection, F_{max}/δ_0, together with the residual deflection after mechanical unloading δ_r, normalized with respect to δ_0, as a function of the testing temperature. As discussed previously, an increase of the stiffness is observed when increasing the temperature, from about 400 to 1150 N/mm, due to microstructure evolutions; in fact, the increase of the testing temperature from 298 to 373 K causes (a) the variation of the volume fraction of residual martensite after unloading and (b) the increase of the stress transformation plateau according to the Clausius–Clapeyron relation.

Furthermore, the microstructure evolution of the washer with increasing the testing temperature is also demonstrated by the values of the residual deflection after unloading, with δ_r/δ_0 ranging from 0.35 at $T_t = 298$ K to 0 at $T_t = 373$ K. The recovery capabilities

of the washers are better illustrated in Figure 17, which reports the pseudoelastic recovery, δ_{PE}, and the shape memory recovery, δ_{SM}, normalized with respect to the maximum deflection δ_0. Figure 17 shows an increase of the pseudoelastic recovery with increasing the temperature, with $\delta_{PE}/\delta_0 = 0.65$ at $T_t = 298$ K and $\delta_{PE}/\delta_0 = 1$ at $T_t = 373$ K. In addition, the residual deflection upon unloading is always recovered after thermal cycle, that is, the shape memory recovery, δ_{SM}, is equal to the residual deflection δ_r.

Figure 18 shows the energetic parameters of the mechanical cycle, that is, the total energy E_T, the recovered energy E_R, and the dissipated energy E_D, as a function of testing temperature T_t. An increase of the total energy is observed with increasing the testing temperature, as a direct consequence of the increase of the stiffness, with values ranging from about 400 mJ at $T_t = 298$ K to about 1200 mJ at $T_t = 373$ K; a similar trend is observed for the recovered energy with values ranging from 200 to 1000 mJ. The dissipated energy E_D shows a nonmonotonic trend with a maximum value of about 200 mJ at room temperature and a minimum value of about 150 mJ at $T_t = 323$ K and a successive slight increase with increasing the testing temperature up to about 180 mJ at $T_t = 373$ K. However, it is worth noting that the larger value of dissipated energy at low temperature is mainly due to the large residual deflection upon unloading, that is, it is observed only in the first loading–unloading cycle, and consequently, it cannot be used in damping applications that involve repeated loading cycles. On the contrary, the dissipated energy at $T_t > 373$ K is expected to be constant during repeated mechanical cycles, as it is obtained with no residual deflections upon unloading.

Finally, it is worth noting that multiple Belleville washers may be used to modify the global functional and/or mechanical responses, and it is a common practice when dealing with classical Belleville washers. In particular, they can be stacked in the same direction, which corresponds to springs in parallel, in an

Figure 17. Pseudoelastic and shape memory deflection recovery normalized with respect to the maximum deflection (δ_{PE}/δ_0 and δ_{SM}/δ_0), as a function of the testing temperature, T_t.

alternating direction, corresponding to springs in series, or in a mixed mode. A parallel stacking arrangement allows to obtain a stiffer joint and, consequently, a higher recovery force if used in actuation application; on the contrary, if using a series stacking arrangement, a lower stiffness is obtained together with a higher deflection recovery. However, much research should be carried out to better understand the thermomechanical behavior of NiTi-based Belleville washers under both static and cyclic loading conditions, as well as to improve the manufacturing process in order to enhance the mechanical and functional properties of the washers.

Conclusion

NiTi-based Belleville springs have been analyzed in this investigation, together with their unique features, due to reversible phase transformation mechanisms. In particular, numerical simulations have been carried out for a preliminary design of the Belleville washer, using a commercial FE software and a special constitutive model for SMAs; the simulations revealed a marked effect of the temperature on the force–deflection curve of the washers, due to the temperature-dependent stress–strain response of the SMA, as well as a loading path-dependent response, that is, they exhibit a hysteretic behavior as a direct consequence of the hysteresis associated with the stress-induced phase transformation mechanisms. After the preliminary numerical simulations, Belleville springs have been manufactured from a commercial pseudoelastic NiTi sheet, by disk shearing, and a successive shape setting, by a thermomechanical process. The thermomechanical response of the manufactured washers, in terms of isothermal force–deflection curve and thermal cycles between phase transition temperatures, has been experimentally analyzed. The results qualitatively confirm the preliminary numerical observations, that is, the washers show a significant effect of the temperature on the characteristic curve as well as a marked hysteretic behavior. However, due to several assumptions and limitations of the adopted constitutive model as well as to the marked modifications of the thermomechanical properties of the alloy after the thermomechanical forming process, a direct comparison between numerical results and experimental measurements cannot be made. As a consequence, FE simulations can be just considered as preliminary studies that allow to define the overall geometric properties of the Belleville washers based on the design needs, but complete experimental tests should be carried out for an accurate knowledge of their thermomechanical response. Furthermore, the experimental results showed that the washers exhibit both pseudoelastic and shape memory recovery capabilities depending on the testing temperature. Due to these interesting properties, NiTi Belleville washers can be used as smart elastic components, that is, with variable and tunable mechanical response depending on the temperature, as well as active elements, that is, they are able to generate forces and/or deflections under thermal cycles between the phase transition temperatures. Furthermore, the hysteretic response of the springs is particularly useful for the realization of vibration and/or seismic absorbers, as demonstrated in previous researches.

References

Auricchio F (2001) A robust integration-algorithm for a finite-strain shape memory alloy superelastic mode. *International Journal of Plasticity* 17: 971–990.

Auricchio F and Taylor RL (1997) Shape-memory alloy: modeling and numerical simulations of the finite-strain superelastic behavior. *Computer Methods in Applied Mechanics and Engineering* 143: 175–194.

Labrecque C, Braunovic M, Terriault P, et al. (1996) Experimental and theoretical evaluation of the behavior of a shape memory alloy Belleville washer under different operating conditions. In: *Proceedings of the annual Holm conference on electrical contacts*, Chicago, IL, 6–20 September 1996, pp.195–204.

Otsuka K and Ren X (2005) Physical metallurgy of Ti-Ni-based shape memory alloys. *Progress in Materials Science* 50(5): 511–678.

Otsuka K and Wayman CM (1998) *Shape Memory Materials*. Cambridge: Cambridge University Press.

Reynaerts D and Van Brussel H (1998) Design aspects of shape memory actuators. *Mechatronics* 8: 635–656.

Saadat S, Salichs J, Noori M, et al. (2002) An overview of vibration and seismic applications of NiTi shape memory alloy. *Smart Materials and Structures* 11: 218–229.

Speicher M, Hodgson DE, DesRoches R, et al. (2009) Shape memory alloy tension/compression device for seismic retrofit of buildings. *Journal of Materials Engineering and Performance* 18(5–6): 746–753.

Spinella I and Dragoni E (2010) Analysis and design of hollow helical springs for shape memory actuators. *Journal of Intelligent Material Systems and Structures* 21: 185–199.

Spinella I, Dragoni E and Stortiero F (2010) Modeling, prototyping, and testing of helical shape memory compression springs with hollow cross section. *Journal of Mechanical Design* 132: 1–9.

Trochu F and Terriault P (1998) Nonlinear modelling of hysteretic material laws by dual Kriging and application. *Computer Methods in Applied Mechanics and Engineering* 151(3–4): 545–558.

Wichelhaus A, Brauchli L, Ball J, et al. (2010) Mechanical behavior and clinical application of nickel-titanium closed-coil springs under different stress levels and mechanical loading cycles. *American Journal of Orthodontics and Dentofacial Orthopedics* 137: 671–678.